Basic Experimental Study on the Flexural Strength of the Beam Web at Square CFT Column - H Shaped Beam Connection

M. LIU
Faculty of Environmental Engineering, the University of Kitakyushu, Japan

M. KIDO
Faculty of Environmental Engineering, the University of Kitakyushu, Japan

K. TSUDA
Faculty of Environmental Engineering, the University of Kitakyushu, Japan

SUMMARY
This paper is about the flexural strength of the beam web connected to concrete filled steel tubular column (from now referred to as CFT column) when the out-of-plane deformation is considered. A simplified strength formula obtained by the mechanism method has been proposed. The purpose of this study is to discuss the effects of test parameters on maximum strength and strain distribution of beam webs. Test parameters are width-to-thickness ratio of column skin plate, presence or absence of scallops and presence or absence of infilled concrete. In specimens with non-scallops, local buckling occurred and the loads decreased slowly. However, the loads of the specimens with scallops decreased suddenly after cracks occurred at the tip of scallop at the bottom flange. The deflections of non-scallops specimens are larger than those with scallops. The maximum strength is larger, when there are non-scallops, the width-to-thickness ratio is smaller and there is infilled concrete.

Keywords: Beam-Column Connection, Steel-Concrete Composite column, Composite beam

1. INTRODUCTION

In the American Northridge earthquake and Hyogoken Nanbu earthquake, brittle failures occurred at the welding connections of the beam ends[1)]. In addition, most brittle failures and cracks which observed near the full penetration welding connections of the through diaphragms and the beam flanges occurred at the lower flanges of the beams in the frame structures composed of square steel tubular columns with H-shaped beams[2)].

To prevent such brittle failures, [The Guideline for Brittle Fracture Resistance at Welded Steel Beam Ends, 2nd Edition (in Japanese)] [1)] (from now referred to as Guidance for Brittle Failure Prevention) was published in Japan. The design and welding construction methods of the connection of beam ends are shown, as well as the equations for evaluating the plastic rotational angle (i.e., the capacity of carrying deformation) of square steel tubular column with H-shaped steel beam.

About the connection of the CFT column and the H-shaped beam, the properties of the connection where the stress of beam flange is transmitted to the column through the diaphragm have been researched by many experimental studies. The strength evaluation method and the restoring force models' characteristics of the connection have been proposed. All of these have been summarized in Chapter4, Part 3 of Concrete-Filled Steel Tubular Structure Design and Construction Guidelines.

On the other hand, the flexural strength of the connection of the steel beam ends can be evaluated by the sum of the flexural strength of each beam flange and beam web. However, when the column is hollow steel column, the out-of-plane deformation occurs at the skin plate of column in which the beam web obsessed, and the bending moment of the beam web transferred to the column becomes smaller. As a result, the flexural strength of beam connection decreases. About the flexural strength of the connection of the square or circular hollow steel column and the beam web, the strength evaluation method has been proposed[4)-8)], so that depending on the width-to-thickness or the radius-to-thickness ratio of steel tube, the flexural strength of the connection of beam web can be evaluated. In addition, because of the out-of-plate deformation of steel tube, the load-transmission efficiency of the beam decreases and deformation capacity of the beam cannot be obtained [9]. The relation between the load-transmission efficiency and the capacity of deformation has been shown in several studies[10)-13)].

When the column is a square CFT, because of the presence of concrete, the out-of-plate deformation of the skin plate of the column can be restrained at the compressive portion of the beam web. However, at the tensile side, the out-of-plate deformation can hardly be restrained [14]. Therefore, the flexural strength of the connection of the square CFT column and the beam web has been calculated by the mechanism method and the evaluation formula which is based on the evaluation formula of the flexural strength when the column is hollow steel column as shown in reference 5 was presented[14]. In addition, the test about the connection of the square CFT column and H-shaped steel beam was carried out with the width-to-thickness ratio as the parameter, and discussion about some analyses on the maximum strength and the distribution of strain at the beam has been presented[15]. However, there are no experimental studies focusing on the flexural strength of the connection of the beam web in the connection of the CFT column and H-shaped steel beam with slabs.

The purpose of this study is to carry out tests about the connection of the square CFT column and the H-shaped steel beam to make sure the effects of the width-to-thickness ratio of CFT column, presence or absence of scallops and presence or absence of infilled concrete on the maximum strength then to analyse the effect of the scallops on the out-of-plate deformation of the steel tube and the distribution of strain at the beam web. In this study, the loading condition of the test is the simple beam condition and the both sides of the column are connected with beams. The both sides of slabs are subjected to compressive force. The loading condition of this test rarely occurs in the actual structure. This study is the basic one that focuses on the out-of-plate deformation of the skin plate of the column and the flexural strength of connection of beam web.

2. TEST PROGRAM

2.1. Outline of test

In this test, the specimens are all the square CFT columns and the square hollow steel column whose size are $\square\!-300\times300\times t_c$ (t_c is the thickness of the steel pipe which is 6mm or 9mm) and slab are connected with the H-shaped beam whose size is $\mathrm{H}-400\times200\times8\times13$. The loading conditions of the test are the simple beam condition and monotonic loading.

As mentioned in Chapter 1, the loading condition used in this test doesn't occur in the actual structure. This study is just a basic research that focuses on the out-of-plate deformation of the column and the flexural strength at the connection of beam webs, for this reason, this loading condition was adopted.

The parameters of this test are 1) the ratio of the width-to-thickness 2) the presence or absence of scallops 3) the presence or absence of infilled concrete. The specimens in this test are named as the different features of each parameter, which are shown as Table 1. The actual dimension of each

Table 1. Test specimens

Name	infilled concrete	Thickness of column tube t_c (mm)	Width-to-thickness ratio (rank)	scallop	Strength of concrete (N/mm^2)	
					column	slab
R50C-PA1.3-NS-S	presence	6	50 (FD)	absence	36.3	27.5
R33C-PA1.3-NS-S		9	33 (FC)		36.3	28.2
R33C-PA1.3-S-S				presence	37.1	28.9
R33S-PA1.3-NS-S	absence			absence	—	28.9

Example of specimen's name

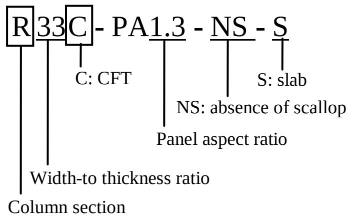

Table 2. Actual dimensions of specimen (Unit: mm)

Name	Thickness of beam flange	Thickness of beam web	Thickness of steel tube	Thickness of diagram
R50C-PA1.3-NS-S	13.14	7.87	5.95	18.97
R33C-PA1.3-NS-S	13.27	7.98	8.99	18.95
R33C-PA1.3-S-S	13.32	7.92	8.99	18.95
R33S-PA1.3-NS-S	13.24	7.83	8.99	19.00

specimen is shown as Table 2.

2.2. Test specimens

Figure 1 shows the shapes of the specimens. The tube of CFT is BCR295, the beam is SN400B and the diaphragm is made of the plate whose thickness is 19mm. The slabs are all made of composite deck plates. The height of the composite deck plate and the composite slab are 50mm and 130mm respectively. The width of the slab is 920mm.The headed studs are used as the shear connectors. The diameter of the studs is 13mm and the length of studs is 80mm. The double rows of studs are placed every 200mm pitches. In addition, the 6ϕ@150 Welded wire meshes are set where 30mm far away from the surface of concrete. Around the slab, the angle steels L-50 × 50 × 6 are installed for receiving composite decks, and the steel plates whose depth and thickness are 130mm and 3.2mm respectively. It should be noted, the beams are the incompletely composite beams.

2.3. Material property

To investigate the material properties of steel, tensile test is performed. Tensile test is carried out by three tensile test pieces (No. JIS1-B), which are cut out from H-shaped steel, diaphragm plate and steel pipe respectively. Table 3 shows the results of tensile test and Figure 2. (a) shows the typical relation between the stress and the strain. By 0.2% offset method about the column, the yield stress is obtained.

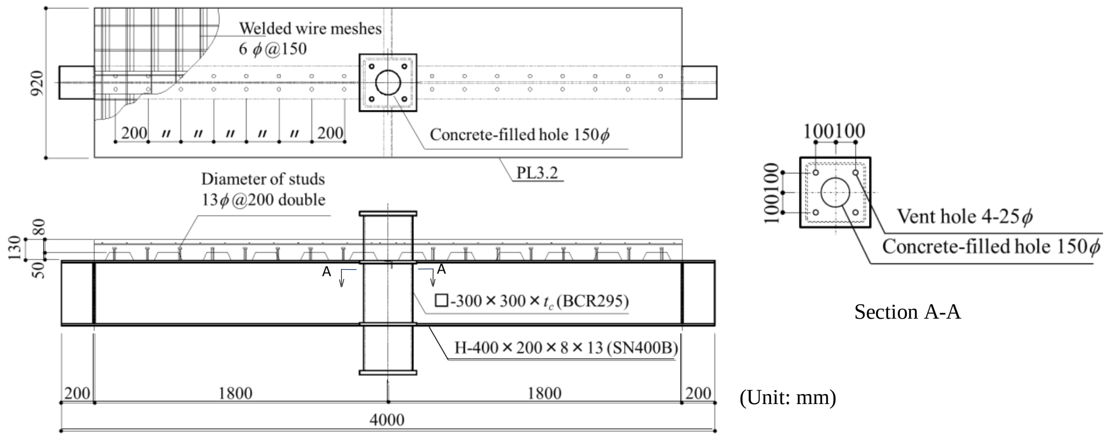

Figure 1. Specimen (CFT column)

Table 3. Results of tensile test

situation	σ_y (N/mm^2)	σ_u (N/mm^2)	σ_y/σ_u (%)	ε_{st} (%)	EL (%)
Beam flange	325	438	74.2	2.63	26.8
Beam web	359	455	78.9	2.77	26.2
Steel tube (t = 6mm)	363	448	81.1	—	25.3
Steel tube (t = 9mm)	328	405	81.0	—	28.0
diaphragm	383	528	72.6	1.91	27.0

σ_y , σ_u : yield stress and tensile strength, σ_y/σ_u : yield ratio
ε_{st}, EL : strain at the begin of strain hardening and elongation at breaking

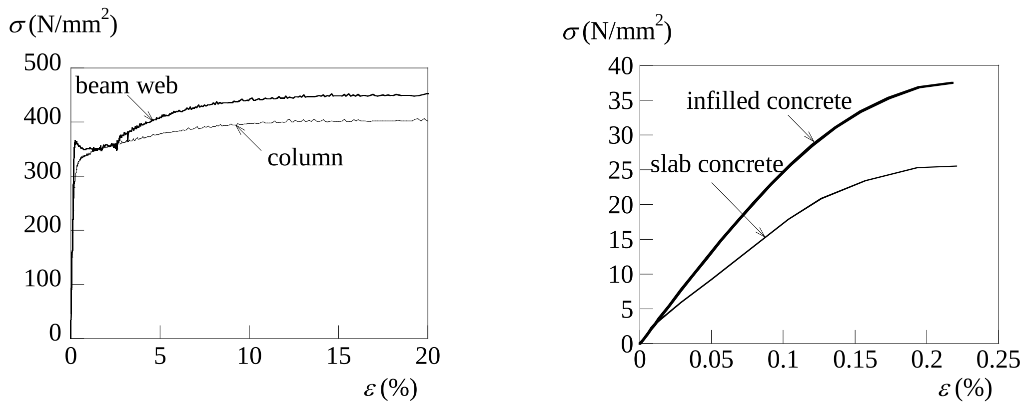

(a) Beam web and steel tube (b) Concrete

Figure 2. Relation of stress-to-strain ratio (example)

Table 4. Preparation of the concrete

Situation (strength)	Water-to-cement ratio (%)	Cement (kg/m^3)	water (kg/m^3)	Fine aggregate (kg/m^3)	Coarse aggregate (kg/m^3)	Admixture (kg/m^3)	Slump (cm)
Column ($30N/mm^2$)	45.0	414	186	742	971	3.73	18
Slab ($18N/mm^2$)	63.0	291	183	869	955	2.62	18

The preparation of the concrete is shown in Table 4. The cylinder compression test of each specimen is carried out. Table 1 shows the concrete compressive strength of each specimen. In addition, the typical relation between the stress and the strain is shown in Figure 2. (b).

2.4. Measurement method

Figure 3 shows the loading apparatus and the method of measurement is shown in Figure 4. The vertical displacements of two points at one end of the beam (v_1, v_2) and a point at the other end of the beam (v_3) are measured (shown as Figure 3). The vertical displacements at left and right ends of the beam (δ_s and δ_n) are calculated by Eq. (1) and Eq. (2) respectively.

$$\delta_s = \frac{v_1 + v_2}{2} \tag{1}$$

$$\delta_n = v_3 + \frac{v_2 - v_1}{2} \tag{2}$$

The column with diaphragm is considered as a rigid body and rotated an angle θ_c around the loading point. The rotational angle θ_c can be calculated by Eq. (3).

$$\theta_c = \sin^{-1}\left(\frac{\delta_s - \delta_n}{D}\right) \tag{3}$$

The rotational angles at left and right sides of the beam (θ_n and θ_s) can be calculated by Eq. (4) and Eq. (5). In which, l_n and l_s are the displacements from the joints to the surface of the column and the subscripts n and s represent the left and right sides respectively.

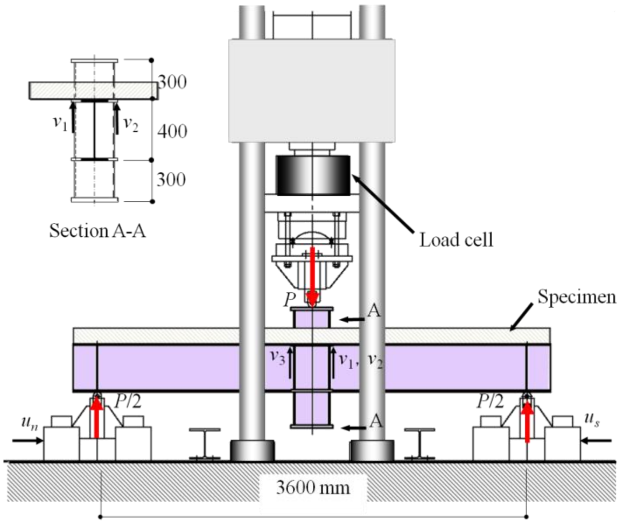

Figure 3. Loading apparatus

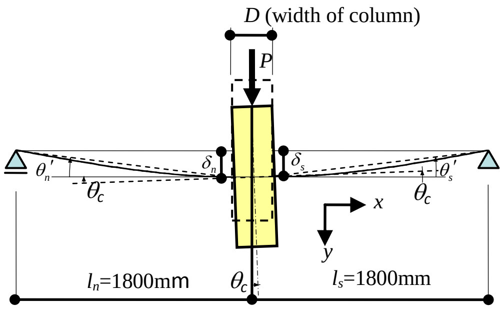

Figure 4. Method of measurement

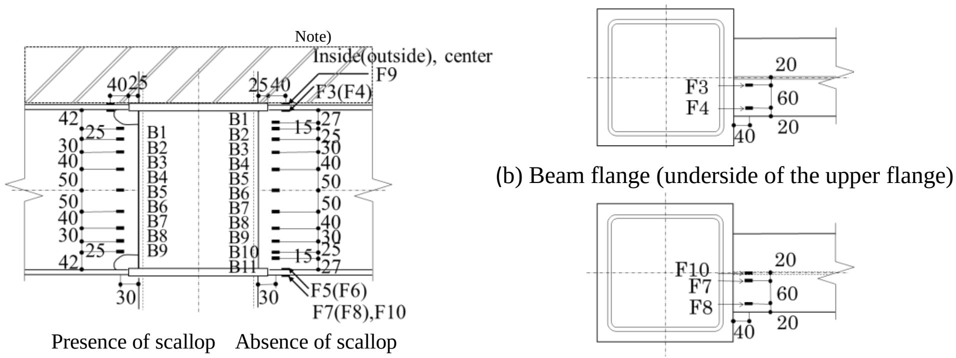

(a) Beam flange and beam web

(b) Beam flange (underside of the upper flange)

(c) Beam flange (underside of the lower flange)

Note) "inside" of beam flange is the position near beam web (the position of F7 in Figure 5.(c)).
"outside" is the end position of beam flange (the position of F8 in Figure 5.(c)).
"center" means the middle of beam flange(the position of F10 in Figure 5.(c)).

Figure 5. Position of stain gauges pasted

$$\theta_n = \theta_n' + \theta_c = \tan^{-1}\frac{\delta_n}{l_n - D/2} + \theta_c \tag{4}$$

$$\theta_s = \theta_s' - \theta_c = \tan^{-1}\frac{\delta_s}{l_s - D/2} - \theta_c \tag{5}$$

In addition, the strains are measured by the strain gauges which are pasted at the flanges and webs of the beams, as well as the skin plates of the columns. The positions where the stain gauges were pasted are shown in Figure 5. It should be noted, the strain gauges are all pasted in the axial direction of each structural member.

3. TEST RESULT

Photo 1.(a) is the photo of the specimen, R33C-PA1.3-NS-S, which is chosen as the standard test body. The specimen with scallops, R33C-PA1.3-S-S, cracked at the lower flange of the beam. Photo 1.(b) and (c) show the crack seen from the side and below. In all the specimens with non-scallops, crack did not occur, but local bucking occurred at the upper flanges of the beams.

3.1. Relation between the load and the slope angle

Table 5 shows the maximum load and the corresponding slope angle of each specimen. Figure 6 shows the relation of the load P and the rotational angle θ. The greater value of deformation between the left and the right side is chosen as the rotational angle. In Table 5, to make a comparison with the standard test body (R33C-PA1.3-NS-S) the ratios of the maximum load between the standard test body and the other specimens, as well as the ratios of the corresponding rotational angle are also listed besides the maximum load and the corresponding rotational angle. Figure 6.(a) ~ (c) show the comparisons between the standard test body (R33C-PA1.3-NS-S) and the other specimens which have differences with the standard test body in the width-thickness ratio, presence or absence of scallop and presence or absence of in-filled concrete respectively.

The specimen whose width-to-thickness is 50 was stopped because of the failure of the jig (thin line in Figure 6(a)). To other specimens, the concrete of slabs crushed at the end of the beams. Once the load dropped, in the specimens with non-scallop, local buckling occurred at the beam flanges and the load decreased slowly (Figure 6.(c)), while crack at the bottom flange of the beam occurred in the specimens with scallops and the load of them decreased rapidly (thin line in Figure 6(b)).

On maximum load, the influence of each parameter is considered. About the differences of the width-thickness ratios (Figure 6(a)), it is easy to know the maximum load of specimen whose width-thickness ratio is 50 is less than the one whose width-thickness ratio is 33(96.1%, Table 5). About the presence or absence of scallop (Figure 6(b)), we can see the maximum load of specimen with scallop is smaller (94.0%, Table 5). About the presence or absence of in-filled concrete (Figure 6(c)), the load of the hollow specimen without filled concrete is smaller than the load of the specimen in-filled concrete (95.2%, Table 5).

(a) Specimen after test
(R33C-PA1.3-NS-S)

(b) Crack occurred in scallop
(R33C-PA1.3-S-S)

(R33C-PA1.3-NS-S)(c) Crack as seen from the underside flange

Photo 1. Specimen after the test

Table 5. Maximum load and corresponding slope angle

Name	Maximum load (kN)	Corresponding rotational angle (rad)	Ratio of other specimen compared with the standard test body (%)	
			Maximum load	Rotational angle
R50C-PA1.3-NS-S	859	0.0451	96.1	1.01
R33C-PA1.3-NS-S	894	0.0447	-	-
R33C-PA1.3-S-S	840	0.0652	94.0	1.46
R33S-PA1.3-NS-S	851	0.0375	95.2	0.84

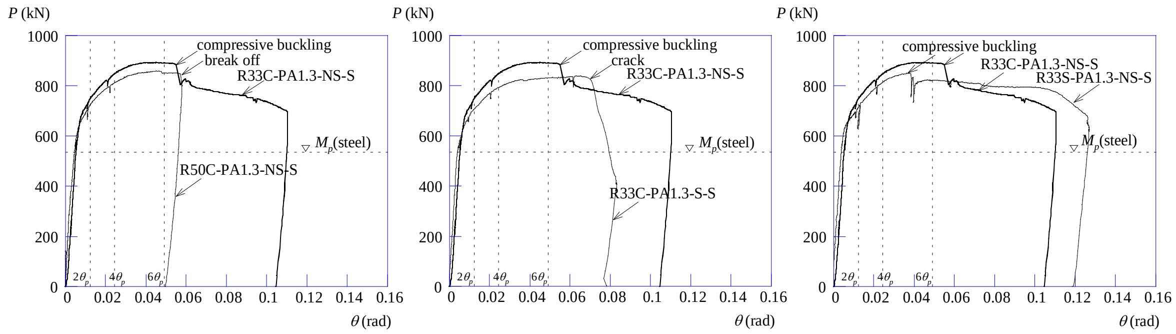

(a) Comparison of width-to-thickness (b) Comparison of presence or absence of scallop (c) Comparison of presence or absence of infilled concrete

Figure 6. Relation between load P and slope angle of beam θ

In addition, the rotational angle corresponding to the maximum load of the specimen with scallop is the largest of all. However, among the specimens with non-scallops, the rotational angle of the specimen as the standard test body whose width-to-thickness ratio is 33 is larger than the others and the rotational angle of the hollow specimen is the smallest.

3.2. Distribution of the strain at beam web

Figure 7 shows the strain distribution of beam web. In detail, Figure 7.(a) and Figure 7.(b) are about the specimens with scallops or not respectively in two situations when the load P equals 50kN in the elastic range and when the deformation is in the plastic range. We assume θ_p is 0.00612rad (the calculated value about the H-shaped steel beam section neglecting the effect of the slab). The distributions of strain when the rotational angle is $2\theta_p$, $4\theta_p$ or $6\theta_p$ respectively are shown in Figure 7. The dotted lines in Figure 7 represent the neutral axes in the elastic range under the Navier's hypothesis. Besides, the strain of the lower side of the beam is larger, while the strain of the upper side can hardly be observed.

In addition, making a comparison between the specimen with scallop and the one with non-scallop, it is easy to find that the strain of the specimen with non-scallop is larger than the other one. When the rotational angle is equal to $6\theta_p$, the maximum of the strain is reached and the strain of the specimens with scallops or not are 2.36% and 1.69% respectively. It is considered that, to the specimen with scallops, the out-of-plate deformation at the skin plate of the columns is much larger, and the strain of the beam webs is smaller.

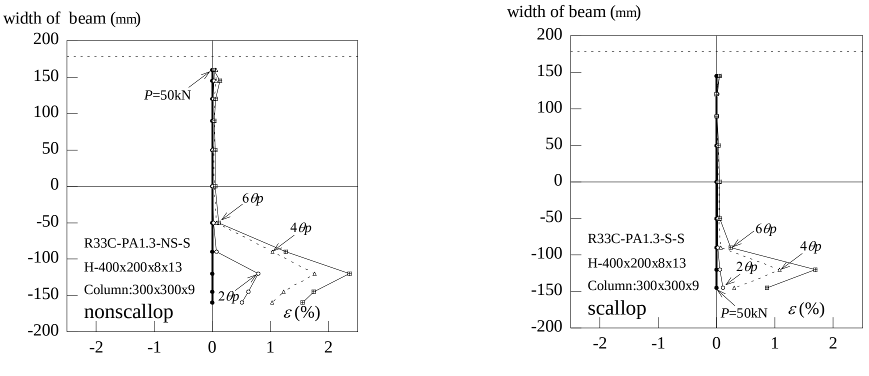

(a) Absence of scallop (b) Presence of scallop

Figure 7. The distribution of strain at beam web

4. CONCLUSIONS

To make sure the effect of the width-to-thickness ratio about CFT column, presence or absence of scallops and presence or absence of infilled concrete with the maximum strength respectively, the test about the connection of the square CFT column and the H-shaped steel beam has been carried out.

(1) About maximum load, the specimen whose width-to-thickness is larger, the specimen with scallop and the specimen with hollow column are smaller than others. The ratios of maximum Strength compared with the standard test body are from 94% to 96.1%.

(2) About the distribution of the strain of the beam web, the specimen with non-scallop is larger than the one with scallop.

This study focuses on the out-of-plane deformation of skin plate of steel column and the flexural strength of connection of beam web. Because the loading condition of this test is not the real condition which exists in fact, we will take more tests under different loading conditions in the future.

ACKNOWLEDGEMENT
This study was assisted by Grant-in-Aid for Scientific Research, MEXT in 2008-2009. In addition, thanks to the Kyoeikogyo Company that produced specimens for this test. At last, thanks to all of the students that tried their best to help with this test.

REFERENCES

The Building Centre of Japan. (2003).The guideline for brittle fracture resistance at welded steel beam ends, 2nd Edition (in Japanese).

The Architectural Institute of Japan Kinki Branch Steel Structural Group. (1997).The test about plastic behaviour of H-shaped beams connected with SHS column (in Japanese).

Architectural Institute of Japan. (2008).The Recommendations for design and construction of concrete filled steel tubular structures (in Japanese).

Morita,K., Ebato, K., Funahasi, A., Kominami, T. and Takayuki S. (1989). Study on structural behaviours of beam-to-column connections: in case corner weld of box column is partial penetration weld (in Japanese). *Journal of Structural Engineering architectural institute of Japan*. **397**, 48-59.

Suita, K. and Tanaka, T. (2000). Flexural strength of beam web to square tube column joints, Steel construction engineering (in Japanese). *Journal of Steel structure.* **7:26**, 51-58.

Tateyama, E., Inoue, K., Sugimoto, S. and Matsumura, H. (1988). Study on ultimate bending strength and deformation capacity of H-shaped beam connected to RHS column with through diaphragms. *Journal of Structural Engineering architectural institute of Japan*. **389**, 109-121.

Tabuchi, M., Sakamoto, S., Kanatani, H., Fujiwara, K. and Kamba, T. (1988). The flexural strength of H-beams welded to RHS-columns (in Japanese). *Journal of Structural Engineering architectural institute of Japan*. **389**, 122-131.

Tanaka, T., Tabuchi, M. and Murakami, H. (2001). Flexural strength of H-beam web connected with circular hollow section columns (in Japanese). *Journal of Constructional Steel*. **9**, 457-464.

Architectural Institute of Japan (AIJ). (2006). Recommendation for Design of Connections in Steel Structures, 1st edition (in Japanese).

Tanaka, A., Masuda, H., Takagi, M. and Hisada, T. (1996). Experimental study on the static characteristics of the WBFW type beam-to-column connections. *Journal of Structural Engineering architectural institute of Japan*. **484**, 121-130.

Masuda, H., Tanaka, A., Qian, G. (1998). A study on the statical characteristics of the WBFW type beam to SHS column connections (in Japanese). *Journal of Structural Engineering architectural institute of Japan*. **509**, 151-158.

Matsumoto, Y., Akiyama, H., Yamada, S. (1999). Relation between deformation capacity of beam at steel beam-to-column connection and joint efficiency (in Japanese). *Journal of Structural Engineering (AIJ)*. **523**, 117-124.

Okada, K., Oh, S. and Yamada, S. (2003). Effect of joint efficiency at beam-to-column connection on ductility capacity of composite beams. *Journal of Structural Engineering architectural institute of Japan*. **573**, 185-192.

Kido, M. and Tsuda, K. (2006). Flexural strength of beam web to concrete filled square steel tubular column joints (in Japanese). *Journal of Structural Engineering architectural institute of Japan*. **602**, 219-226.

Kido, M. (2010). Experimental Study on Flexural Strength of Beam Web to Concrete Filled Square Steel Tubular Column Joints Effect of the depth-thickness ratio of the steel tube (in Japanese). *Summaries of technical papers of annual meeting architectural institute of Japan*. 1249-1250.